Fire modulates millennial plant community assembly

Pablo Valgañón[1,2,*], **Alessio Cardillo**[3,4,2,*], **Ana Cano-Herranz**[3], **Hugo Sáiz**[5], **Adam T. Clark**[6], **David García-Callejas**[7], **Lena Neuenkamp**[8], **Cristina Ramos-Capón**[1], **Penelope González-Sampériz**[1], **and Graciela Gil-Romera**[1,*]

[1]Pyrenean Institute of Ecology – (IPE – CSIC), Campus Aula Dei, E-50059, Zaragoza, Spain
[2]GOTHAM Lab – Institute for Biocomputation and Physics of Complex Systems (BIFI), University of Zaragoza, E-50018 Zaragoza, Spain
[3]Department of Condensed Matter Physics, University of Barcelona, E-08028 Barcelona, Spain
[4]University of Barcelona Institute for Complex Systems (UBICS), University of Barcelona, E-08028 Barcelona, Spain
[5]Departamento de Ciencias Agrarias y Medio Natural, Escuela Politécnica Superior, Instituto Universitario de Investigación en Ciencias Ambientales de Aragón, Universidad de Zaragoza, Huesca, Spain
[6]Department of Biology, University of Graz, Graz, Austria
[7]Departament de Biologia Animal, Biologia Vegetal i Ecologia Facultat de Biociencies – Universitat Autònoma de Barcelona, Barcelona, Spain
[8]Faculty of Biology, University of Bielefeld, Universitätße. 25, Bielefeld 33615, Germany
[*]graciela.gil@ipe.csic.es, pvalganon@ipe.csic.es, alessio.cardillo@ub.edu

ABSTRACT

How ecological communities maintain resilience under recurrent disturbance remains unclear because the processes governing persistence often unfold over centuries to millennia. Using fossil pollen and charcoal records spanning up to 14,000 years from mountain ecosystems in Europe and Africa, we reconstructed temporal networks of community predictability to investigate the role of fire in long-term plant community assembly. Across both records, high-fire periods produced denser and more centralised communities dominated by a small number of highly connected taxa, whereas low-fire periods promoted more differentiated structures consistent with niche partitioning. Fire thus repeatedly reorganised communities along a continuum from differentiated to synchronised assembly modes. Despite these pronounced shifts, communities retained a robust giant connected component throughout the records, indicating persistent whole-community coherence. Our results suggest that long-term resilience arises not from compositional stability but from the capacity of communities to reorganise their internal relationships while maintaining an integrated architecture. This framework identifies mechanisms linking disturbance, community assembly and resilience across millennial timescales and provides a baseline for assessing ecosystem responses to ongoing global change.

1 Introduction

Understanding the persistence and dynamics of ecological communities over long timescales represents a fundamental challenge in modern ecology[1]. As anthropogenic pressures push the Earth system beyond its safe operating boundaries[2], identifying the mechanisms that allow communities to remain resilient to severe disturbances has become an urgent priority. In such context, fire has been identified as a major disturbance influencing both ecosystem resilience and biodiversity loss[3]. Fire is a major evolutionary and ecological force with profound consequences for biodiversity, ecosystem functioning, and several planetary processes, including biogeochemical, hydrological, and atmospheric cycles[4]. Although often considered primarily through its immediate social and economic impacts, fire is also a powerful driver of plant community assembly, frequently acting as a selective force that rivals or exceeds other environmental constraints[5–8]. By filtering species according to their tolerance and adaptive responses to disturbance, recurrent fire regimes can shape not only community composition but also the extent to which taxa respond similarly to environmental change. When species are subjected to a common and pervasive selective pressure, their dynamics may become increasingly coordinated, as populations track the same environmental driver through time. Under such conditions, changes in one taxon may contain information about the future behaviour of others. By contrast, when disturbance pressure is weaker, a broader range of ecological strategies can persist, allowing taxa to respond more independently to environmental and biotic constraints. These contrasting situations imply differences in community assembly rules[9] and thus in community-wide predictability, defined here as the degree to which past changes in one taxon improve forecasts of future changes in another[10,11]. Consequently, fire regimes may influence the amount of predictive information shared among taxa. Communities assembled under strong and recurrent fire filtering are expected to exhibit greater predictability because

species respond to a common driver, whereas communities experiencing weaker fire pressure may display more individualistic dynamics and lower levels of shared predictability.

While short-term studies offer critical insights into community dynamics, they frequently miss the slow dynamics, feedback loops, and legacy effects that define ecosystems over centuries and millennia[12]. In estimating the role of fire on centennial to millennial timescales and to formulate robust ecological forecasts, it is crucial then to track baseline conditions and long-term ecosystem dynamics of community resilience[13,14]. The long-term persistence of plant communities depends not just on their ability to resist disturbance, but on their capacity to reorganise while retaining essential structure and function[15] – a capacity governed by the interplay between stabilising and destabilising mechanisms arising from a combination of biotic and environmental drivers[1,16]. Central to these dynamics is niche partitioning, whereby species occupy distinct functional roles and experience stronger net intraspecific than interspecific competition, thereby reducing competitive exclusion and promoting species coexistence[16]. Because occupying distinct functional roles often entails differing responses to environmental drivers, such functional differentiation also tends to reduce covariance among species' responses to perturbations, although complete independence is rare, as many taxa remain exposed to common environmental fluctuations[17]. This partial decoupling promotes community stability by distributing risk across species and reducing the likelihood of synchronous declines[18,19]. Conversely, a single environmental driver that becomes strong or pervasive enough can override this heterogeneity, overwhelming the conditions that would otherwise allow taxa to partition their responses and compelling species into functional redundancy. Under such conditions, taxa respond synchronously to the shared pressure, reducing a community's capacity to buffer perturbations and increasing its susceptibility to critical transitions[20,21].

This capacity has often been studied through the reorganisation of species interaction networks, whereby shifting patterns of interaction among species , or interaction rewiring, can buffer ecosystem function against disturbance even as the specific relationships linking individual species change[22]. While such studies typically rely on direct observation of species interactions, an analogous form of reorganisation can be traced through causal networks, *i.e.*, identifying statistical predictability among taxa. In these, a link denotes the degree to which the past dynamics of one species helps forecast the future dynamics of another[23]. This methodology offers a means of tracking community-level reorganisation in systems, such as the palaeoecological record, where direct interactions cannot be observed but their statistical signature persists in the co-dynamics of species over time.

In this study, we hypothesise that fire activity acts as a primary modulating force in the assembly of high-altitude plant communities at millennial scales, functioning as a selective pressure that reorganises the predictability relationships linking taxa within these communities, shifting them between two contrasting states. Under strong environmental filtering associated with recurrent fire activity, we expect communities to shift toward the synchronised end of this continuum, reflected in more centralised and tightly coupled predictability relationships; under weaker fire influence, we expect a return toward more distributed, individualistic, dynamics characterised by greater asynchrony among taxa. By examining long-term changes in this structure, we aim to assess how fire-mediated assembly processes influence community stability and ecosystem organisation through time.

The trajectory that we investigate partly spans the transition from the deglaciation period, at 13.7 thousand years calibrated before present (ka BP), through the Holocene onset at 11.7 ka BP, to the present day, focusing on high-altitude subalpine (Basa de la Mora – BSM – Pyrenees, Spain) and afroalpine (Garba Guracha – GGU – Bale Mountains, Ethiopia) ecosystems (Fig. 1). These mountain regions serve as critical natural laboratories and provide essential ecosystem services to millions of people – particularly in Africa. They are also biodiversity hotspots that have served as floral refugia, since the Quaternary glaciations to our days[24]. Yet they are now among the environments most threatened by global warming and land-use change[25].

We move beyond individualistic species-response models to examine how whole community properties emerge and persist through time. Our fundamental units of analysis are individual fossil pollen taxa tracked through successive samples within each sedimentary record, allowing us to reconstruct temporal dependencies among taxa over the last 14,000 years. By applying causal inference – specifically Granger Causality[23] – to continuous fossil pollen and charcoal Holocene records, we reconstruct time-varying predictability relationships through high-resolution palynological data from two high-altitude records split into several *periods* (see Methods). A link in these networks denotes a statistically significant predictive relationship where the past values of one taxon provide information that significantly improves the prediction of another's future state, beyond what can be forecast from that taxon's own history alone. Negative links are interpreted as signatures of the individualistic, compensatory dynamics associated with niche differentiation, whereas positive links indicate the synchronised dynamics expected when a shared driver dominates. As functional strategies are ultimately expressed through the temporal dynamics of the taxa performing them, recurring predictability patterns of this kind offer indirect evidence of the assembly processes shaping community structure.

Our study quantifies the transient dynamics of fire history on community assembly over millennial scales, providing a pioneering, quantitative bridge between neo- and palaeoecological sciences.

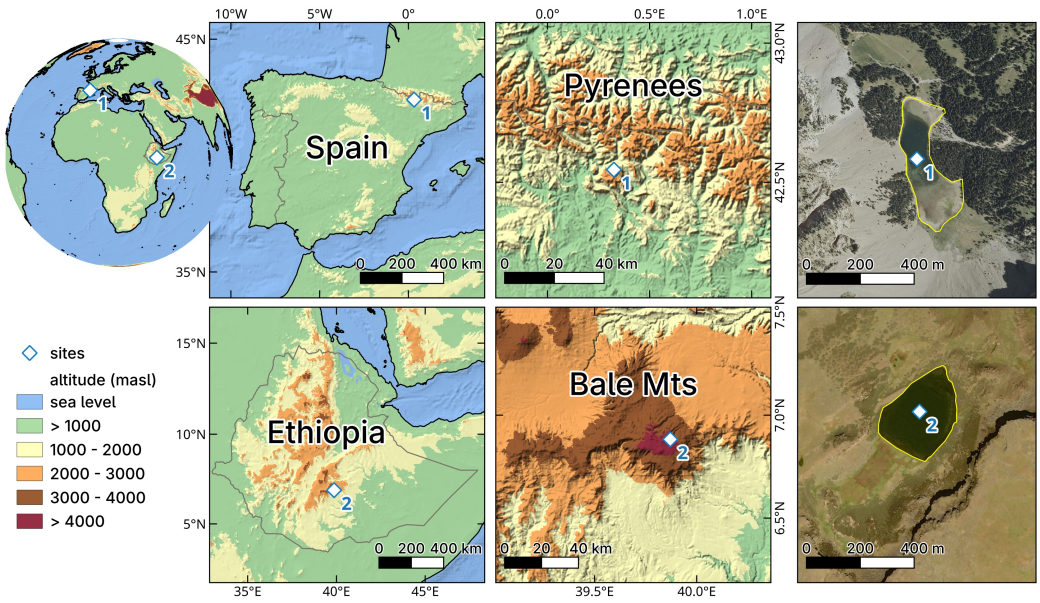

Figure 1. Geographical location of the two sites considered: Basa de la Mora (BSM, Spain) and Garba Guracha (GGU, Ethiopia). For each site, we display their location at country, regional, and local scale.

2 Results and discussion

We track predictability relationships from two high-altitude records under contrasting fire regimes defined according to charcoal-derived fire-activity anomalies (z-scores). The BSM record (1913 m a.s.l.) contains three fire-regime periods: high fire activity (period 1), low fire activity (period 2), and intermediate fire activity (period 3)[26]. The GGU (3940 m a.s.l.) record was divided into four periods: low fire activity (periods 1 and 3) and high fire activity (periods 2 and 4)[27](see Methods; Tab. 1 and Fig. 2).

Our analysis of millennial-scale plant community assembly reveals that community reorganization cannot be explained solely by species-specific environmental tolerances. Rather, we found that the predictive dependencies linking taxa within Granger-causal networks are governed by fire-mediated assembly processes (see Methods; Tab. 1 and Fig. 2).

We examine these networks at two levels of resolution: first among individual taxa, and second among coarse-grained groups aggregating taxa into broader, established ecological communities[28,29]. As detailed in the Methods, coarse-grained networks allow us to map the complex web of Granger-causal links onto functional groups, revealing how the overall ecosystem architecture reorganises functionally across millennial timescales. This dynamic rewiring allows taxa to persist by shifting between distinct assembly modes based on the intensity of environmental stress.

We characterise this reorganisation using five complementary network metrics (see Methods): overall connectivity, captured by the number of significant links (E) and the average degree ($\langle k \rangle$); the percentage of negative links (f_-), reflecting the relative strength of niche partitioning; the Giant Connected Component (GCC), capturing the overall structural integration of the network; and the out-degree of individual taxa, identifying key hub taxa. Together, these metrics allow us to track how fire intensity shifts the ecosystem between decentralised assembly, where predictive influence is spread across many taxa, and synchronised, hub-dominated configurations, where a few taxa disproportionately drive the community's predictive structure. Together, connectivity ($\langle k \rangle$), percentage of negative links (f_-), GCC and out-degree allow us to track: 1) how fire intensity shifts the ecosystem between decentralised assembly, where predictive influence is spread across many taxa, and 2) synchronised, hub-dominated configurations, where a few taxa disproportionately drive the community's predictive structure.

2.1 The shape of millennial timescales predictive relationships between plant communities.

Patterns of predictive relationships among taxa, reconstructed from the BSM and GGU records using Granger Causality, exhibit a temporal reorganisation that closely aligns with shifts in fire disturbance regimes (Tab. 1). Because a link in these networks indicates that one taxon's past dynamics help forecast another's future state, network connectivity – captured by the number of links (E) and average degree ($\langle k \rangle$) – offers a direct measure of how predictable community dynamics are as a whole: more connected networks indicate that many taxa's trajectories are mutually informative, whereas less connected networks indicate that taxa fluctuate comparatively independently of one another. Across both study sites, fire activity has acted as a driver of network connectivity, as periods characterised by elevated fire intensity (periods 1 and 3 in BSM and periods 2 and 4

Table 1. Topological properties of the inferred causality networks obtained from the Basa de la Mora and Garba Guracha sites across different time periods. For each site and each snapshot, we report its duration, the fire anomaly (indicated by its average charcoal record), the number of nodes (N), of links (E) and of self loops (E_0), the percentage of negative links (f_-), the relative size of the Giant Connected Component (GCC), and the average degree ($\langle k \rangle$) for both the original and the coarse networks.

Period ID	Duration (ka BP)	Fire	Charcoal Avg. (z-score)	N		E		E_0	$\langle k \rangle$		GCC		f_- (%)	
				original	coarse	original	coarse	coarse	original	coarse	original	coarse	original	coarse
Basa de la Mora – 140 samples – 1913 m a.s.l.														
1	9.8 – 6.2	High	0.41	63	8	236	55	6	3.74	6.87	0.98	1.00	22.9	36.3
2	6.2 – 3.8	Low	-0.74	60	8	151	40	6	2.51	5.00	0.93	1.00	39.7	46.8
3	3.8 – Pres.	Medium	-0.44	70	8	161	49	6	2.30	6.13	0.99	1.00	32.3	40.5
Garba Guracha – 301 samples – 3950 m a.s.l.														
1	13.6 – 11.1	Low	-0.39	43	6	73	24	3	1.70	4.00	0.95	1.00	50.7	55.3
2	11.1 – 6.8	High	0.80	62	7	118	31	4	1.90	4.43	0.98	1.00	39.8	47.9
3	6.8 – 2.2	Low	-0.27	67	7	135	34	3	2.01	4.86	0.88	1.00	44.4	50.0
4	2.2 – Pres.	High	0.47	79	7	202	31	5	2.56	4.43	0.97	0.86	29.7	41.2

in GGU) consistently display a higher number of links (E) and average degree ($\langle k \rangle$) compared to low-fire periods (period 2 in BSM and 1 and 3 in GGU)).

In BSM, connectivity peaked during period 1, spanning 9.8-6.2 ka BP, in the presence of high fire activity, with 236 links and $\langle k \rangle = 3.74$, before contracting to 151 links and $\langle k \rangle = 2.51$ during the subsequent low-fire period (6.2-3.8 ka BP) (Tab. 1). A more pronounced transition occurred in GGU, where the initial low-fire period 1 (13.6-11.1 ka BP) featured a less connected network of only 73 links ($\langle k \rangle = 1.70$). Connectivity surged during the high-fire activity period 2 (11.1-6.8 ka BP) to 118 links and $\langle k \rangle = 1.90$, eventually reaching its maximum of 202 links ($\langle k \rangle = 2.56$) in the final millennium (period 4). This pattern suggests that fire acts as a strong, shared environmental filter in both records: as more taxa are forced to respond to the same recurring disturbance, their abundances become more mutually predictive, overriding individualistic niche dynamics and compelling diverse taxa to respond as a synchronised whole. Conversely, the less connected networks of low-fire periods imply that, in the absence of this common forcing, taxa track local micro-environmental conditions more individualistically – a decentralised architecture governed by niche partitioning and functional independence rather than shared environmental response.

Beyond raw connectivity, the GCC – which captures whole-community integration rather than link density – remained generally robust at both sites (typically $> 88\%$) throughout the record (Tab. 1). Ecologically, a large GCC indicates that most taxa are embedded within a common web of dependencies, such that community dynamics remain integrated at the whole-system level even when individual links are gained or lost. The persistence of a large GCC therefore suggests that community organisation was broadly maintained despite shifts in fire regime intensity and changing environmental conditions. At BSM, this integration was particularly stable, ranging between 93% and 99% across high-, low-, and intermediate-fire periods. GGU exhibited more dramatic temporal variation: although its proportionally smallest GCC (88%) occurs in period 3 rather than period 1, the latter was characterised by substantially fewer taxa and a markedly reduced connected component. Importantly, this pattern cannot be attributed solely to lower taxonomic richness. Rather, a smaller fraction of the taxa present were incorporated into the dominant network cluster, indicating weaker system-wide integration. This early fragmentation during the initial, pre-Holocene phase that corresponds with a post-glacial environment (14 –11 ka BP), suggests that the plant community inhabiting this recently deglaciated, high-altitude landscape was not only species-poor, but also organised into a relatively loose assemblage of dependencies rather than a tight, cohesive system. During this cool and dry period[30,31], low fire activity allowed niche-driven processes and functional independence to prevail, resulting in a network architecture with only 73 links and a low average degree (Tab. 1). This lack of high-level integration in the early stages of community assembly – where taxa responded individualistically to micro-environmental filters – implies that predictive dependencies among taxa were initially fragmented into isolated clusters, before reorganising into densely interconnected assembly modes characteristic of periods of elevated environmental stress. The subsequent increase in taxon richness, predictive links, and cohesion in GGU therefore demonstrates that, while communities maintain a predictive structural persistence as a whole, the level of internal connectivity is highly sensitive to external abiotic filters, with fire forcing taxa into more synchronised modes of response.

Ultimately, the persistence of a robust GCC across both records implies that, while fire activity may rewire the community's internal predictive structure – shifting the balance between niche-driven independence and environmentally driven synchrony – plant communities maintain their functional integrity as a single, integrated network over long timescales.

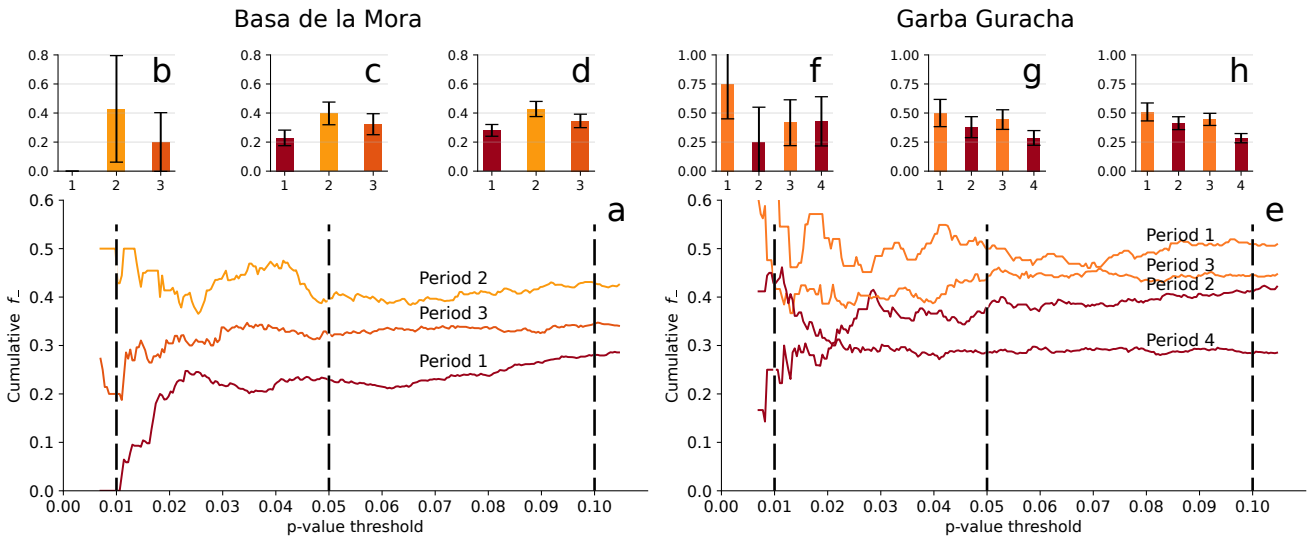

Figure 2. **a** Percentage of negative links f_- found depending on set p-value thresholds chosen for selecting the significant causal links, for periods 1-3 in BSM and **e** periods 1-4 in GGU. **b-d** Percentage of negative links for the p-value thresholds 0.01, 0.05 and 0.10 respectively for the BSM and **f-h** the GGU datasets. The error bars are estimated assuming a binomial distribution with probability f_- and count E (the number of significant links), with a 95% confidence interval. The hue of the bar denotes the fire anomalies intensity for that period, with darker shades representing higher fire intensities.

2.2 The effect of fire on environmentally-driven synchrony and niche-driven functional independence.

The proportion of negative predictive links, f_- – *i.e.*, the fraction of the number of links, E, for which an increase in a taxon's past pollen abundance is followed by a decrease in the abundance of another taxon – varies significantly with changing fire regimes (Tab. 1 and Fig. 2). This metric captures an aspect of network organisation distinct from connectivity: whereas E and $\langle k \rangle$ describe the amount of significant predictive relationships, f_- characterises the balance between antagonistic and synchronous relationships among those connections. Changes in f_- are therefore not a direct consequence of changes in connectivity, and provide additional information about the structure of community dynamics. This distinction is reflected in the coarse-grained networks, which show a clear inverse relationship between fire activity and f_-: periods of lower fire activity were characterised by a significantly higher proportion of negative links, reaching 39.7% in BSM (6.2–3.8 ka BP) and 50.7% and 44.4% in GGU (13.6–11.1 and 6.8–2.2 ka BP, respectively). Ecologically, a higher proportion of negative links suggests that taxa were less tightly coupled in their temporal dynamics, responding to contrasting or asynchronous drivers rather than a shared one. In this context, negative links can be interpreted as signatures of niche partitioning and functional independence, reflecting communities in which predictive relationships over long timescales are maintained through differentiated ecological strategies rather than a common response to prevailing environmental conditions. These results remain consistent across different significance thresholds (p-values) for link selection (Fig. 2), supporting the conclusion that fire activity exerts a strong effect on the organisation and sign of predictive relationships between taxa. This niche-partitioning process finds a natural parallel in modern coexistence theory, where the prevalence of negative links during fire-free periods can be read as a coarse signature of stabilising niche differences – a necessary, though not on its own sufficient, condition for stable coexistence[32,33].

Conversely, high-intensity fire regimes trigger a collapse in negative links, which dropped to 22.9% and 32.3% in BSM (Fig. 3) and to 39.8% and 29.7% in GGU (Fig. 4). This pronounced shift toward a positive-link-dominated architecture within the coarse-grained networks suggests that extreme fire-driven environmental filtering acts as a powerful synchronising force, overriding internal biotic niche differentiation and compelling diverse taxa to respond as an intertwined whole as they share vulnerabilities and resources under the same dominant abiotic pressures. In terms of the underlying Granger Causality framework, the past state of one taxon becomes highly predictive of the future state of others, as the entire community moves along a shared trajectory of recovery or decline dictated by these external drivers.

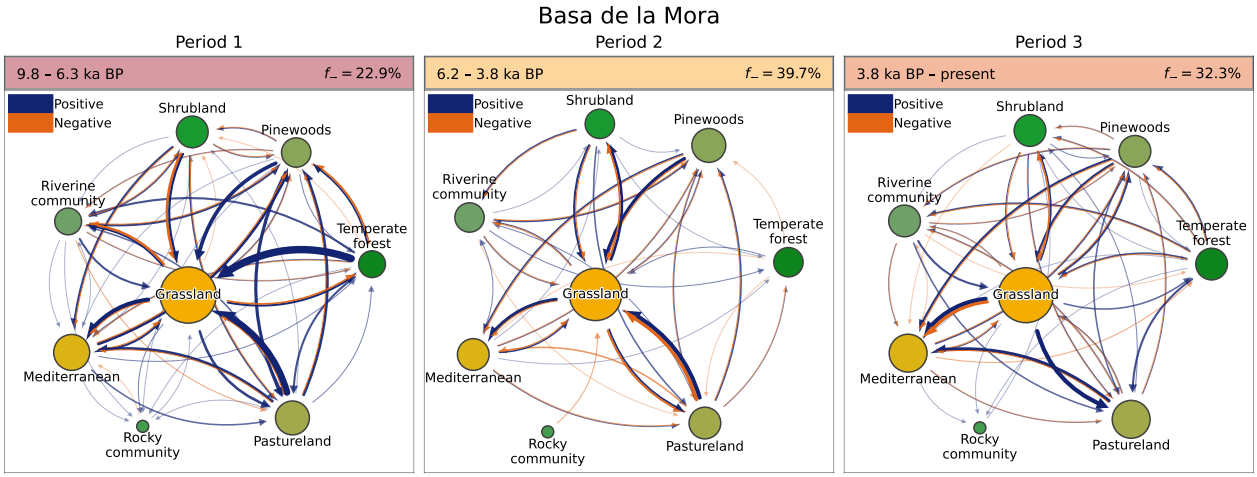

Figure 3. Coarse-grained causal networks of the BSM site for periods 1-3. Each node represents a functional community of taxa, classified in Sec. 2 of the Supplementary Materials. The size of the node represents the number of taxa present in that community and period, and the arrows between groups represent the number of directed positive (blue) and negative (orange) significant causal relationships (below the $p = 0.05$ threshold) between pairs of taxa belonging to them. The direction of the causal links is given by the arrowhead (when arrowheads are not visible, the counter-clockwise direction of the curve defines the flow direction). At the top of each panel the age and percentage of negative links (f_-) is indicated, with darker shades of colour representing higher fire intensity periods.

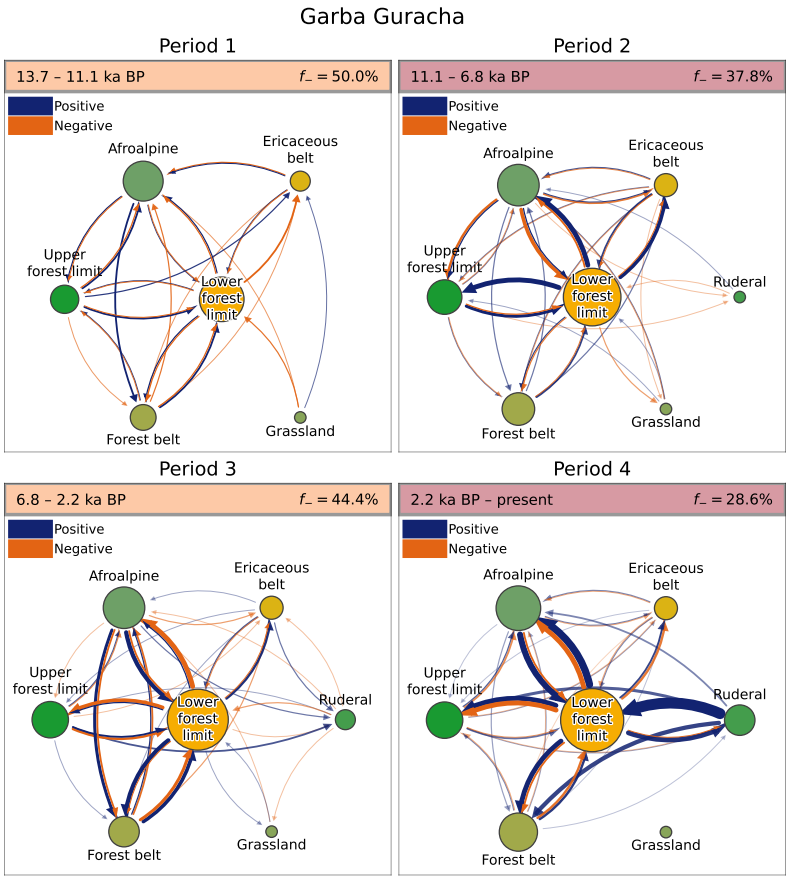

Figure 4. Coarse-grained causal networks of the GGU site for periods 1-4. See the caption of Fig. 3 for the details.

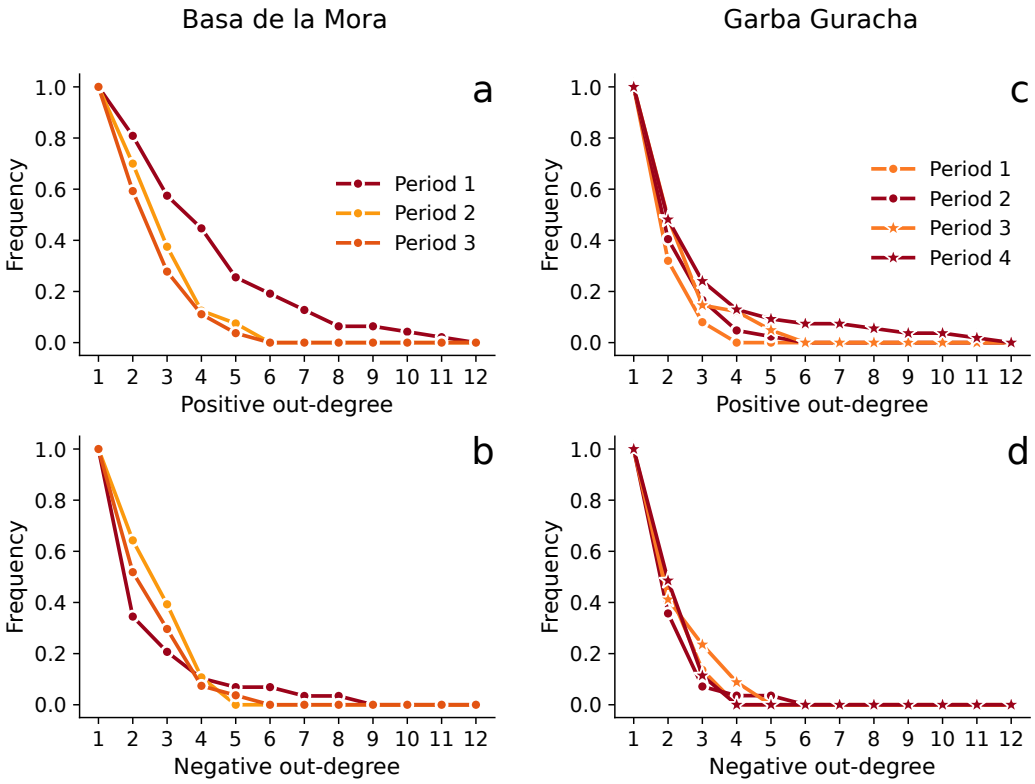

Figure 5. Cumulative degree distributions of the nodes from the BSM **a**, **b** and GGU **c**, **d** networks. The frequency represents the proportion of nodes in the network with (positive **a**, **c** or negative **b**, **d**) degree greater than or equal to each value. Higher fire intensity periods are represented by a darker shade of color.

Shifts in out-degree frequencies (Fig. 5) reinforce this pattern. As introduced above, a taxon's out-degree reflects the number of other taxa whose future dynamics can be predicted by its past values, and can therefore be read as a proxy for its influence – or its responsiveness – within the community, for instance by responding faster to ecological perturbations such as wildfires[34]. During low-fire periods, this influence was evenly distributed across many taxa, producing a flatter out-degree distribution consistent with a decentralised, niche-structured architecture (Fig. 5). Conversely, high-fire periods were dominated by a small number of hub taxa with disproportionately high out-degrees (Fig. 5), acting as key predictive nodes for the wider community and coinciding with its synchronised recovery or decline. Together with the collapse in f_{-}, this hub-dominated topology indicates that intense fire disturbance concentrates predictive influence in a small subset of taxa, rather than distributing it broadly across the community as under weaker fire regimes.

Taken together, our results identify fire as a long-term regulator of community assembly, shifting plant communities between highly synchronised states dominated by shared abiotic constraints and more differentiated states in which taxa respond more independently to environmental variation.

2.3 Resilient response of key communities and taxa

Our analysis of taxon turnover and the persistence of predictive dependencies (see the Methods and Sec. 4 of the Supplementary Materials) shows that, even when the same taxa remain present for millennia, the structure of community organisation is far from static. At its core, this temporal reorganisation reflects the action of environmental filtering on communities exposed to recurrent disturbance, a process well established at ecological timescales but rarely traced continuously over millennial periods. What our approach adds is the ability to follow this process directly through changes in predictive dependencies among taxa, rather than inferring it solely from shifts in species composition or trait turnover. We show that the structure of predictive dependencies among taxa, in two distant alpine ecosystems, changes systematically with shifts in fire regimes, providing a direct temporal signature of changing assembly processes. We suggest that, in these alpine environments, resilience under high-intensity fire regimes is maintained through a reorganisation of community assembly processes. As extreme abiotic filtering intensifies, it overrides internal biotic niche differentiation, leading taxa to exhibit increasingly synchronous responses to environmental forcing. The resulting whole-community synchrony reflects a cohesive system sharing both resources and vulnerabilities.

This hub-dominated topology – in which a few taxa, such as the 'Lower forest limit' in GGU or 'Grasslands' in BSM, exert disproportionate influence during high-fire periods – points to a specific mechanism behind the whole-community coherence captured by the GCC. Rather than every taxon contributing equally to the network's predictive structure, a small subset appears to anchor it, becoming disproportionately predictive of, and possibly driving, the wider community's trajectory while the individual influence of most other taxa is diluted. Whether this predictive dominance reflects these taxa's own fire tolerance, faster post-fire recovery, or some other trait advantage remains an open question. We hypothesise that such taxa exhibit faster post-fire responses, acting as central nodes around which the rest of the community reorganises during disturbance, such that coherence at the whole-network level is preserved even as individual predictive relationships turnover; testing this hypothesis directly would, however, require finer temporal and taxonomic resolution than that available here.

Studies on coexistence theory and community assembly have long emphasised that the persistence of species within a local pool is a dynamic process governed by the interplay between stabilising niche differences and relative fitness differences[35,36]. While traditional ecological models often treat environmental and biotic filters as independent or sequential stages, contemporary theory posits that stable coexistence occurs only when stabilising niche differences – such as resource partitioning, host-specific natural enemies, or the storage effect – are large enough to overcome the relative fitness differences that would otherwise lead to competitive exclusion. In our methodological framework, the proportion of negative links can be read as a coarse, temporal signature of this balance: periods in which negative predictive links prevail are consistent with stabilising differences being strong enough to sustain differentiated, compensatory dynamics among taxa; whereas their collapse under intense fire suggests these differences are being overridden by a shared, dominant driver. This theoretical lens therefore provides a robust foundation for the structural reorganisation observed in these high-altitude ecosystems: community structure is not a fixed architecture but a flexible configuration shifting along the same synchronised-to-differentiated continuum in response to external forcing. Taken together with the persistence of a robust GCC across both records (Sec. 2.1), these results suggest that the resilience of these ecosystems is tied to their ability to maintain whole-community coherence through such structural transitions, preventing a total collapse of the network's predictive structure even under extreme disturbance regimes.

Identifying these hub taxa and assembly modes offers a quantitative basis for ecological forecasting and for designing conservation measures that buffer communities against critical transitions in a rapidly changing world. Across both records, the persistence of a robust GCC together with shifting connectivity, proportion of negative links, and out-degree distributions indicates that these mountain communities have repeatedly absorbed millennial-scale changes in fire regime without losing whole-community coherence – a buffering capacity that should not, however, be taken for granted under anthropogenic pressure. As ecosystems are pushed beyond their safe operating boundaries, a simplification of these networks – particularly the loss of niche partitioning during low-disturbance phases – may erode the structural flexibility that has historically allowed these communities to persist, with a corresponding risk to the ecosystem services they support.

By characterising the baseline conditions of ecosystem complexity prior to the 'Great Acceleration', our approach provides a quantitative framework for assessing how current and future disturbances might reorganise these communities, in line with recent developments in community ecology[37]. In this light, conservation policies should account for internal community architecture – prioritising taxa that maintain connectivity or drive recovery – rather than focusing on individual species protection alone. Ultimately, understanding how long-term persistence is achieved through this predictive flexibility offers a bridge between palaeo- and neo-ecological sciences, providing a more robust basis for ecological forecasting in a rapidly changing world.

Methods

Nature of the data and study cases considered

Plant community composition was reconstructed using fossil palynological assemblages, whereas fire dynamics were inferred from sedimentary macro-charcoal particles. Our analyses drew upon high-resolution, continuous, sedimentary sequences previously retrieved from two geographically distinct natural laboratories, the lakes Basa de la Mora (BSM) in the Central Pyrenees, Spain (1913 m a.s.l.)[38], and Garba Guracha (GGU) in the Bale Mountains, Ethiopia (3950 m a.s.l.)[39]. Both sediment records were dated, depth-age modelled, and analysed by the Quaternary Palaeoenvironment group at IPE-CSIC.

Taxonomic resolution for fossil pollen is typically constrained to the genus or family level, implying that we can derive not so much information on species traits within community response. Thus, we classified pollen assemblages into functional plant communities based on established regional floristic frameworks: the works of Villar *et al.*[28,40] for the subalpine Pyrenean record, and of Miehe *et al.*[41] for the afromontane Ethiopian sequence. Aquatic taxa were excluded from the final datasets, as their dynamics are primarily governed by local limnological conditions rather than the broader upland community assembly processes we aimed to quantify.

*Basa de la Mora (*BSM*)*

Basa de la Mora is a proglacial basin situated in the Cotiella Massif (Central Pyrenees, Spain). The site occupies a critical ecotonal position influenced by Mediterranean climatic patterns, characterized by seasonal precipitation peaks and a mean temperature range of 0.5 °C to 15 °C. The surrounding current vegetation exhibits a complex mosaic of altitudinal zonation:

Lowlands and Montane Belt : Dominated by riparian forests (*Fraxinus excelsior* L., *Populus spp.*) and mixed montane woodlands featuring *Pinus sylvestris* L., *Fagus sylvatica* L., and *Quercus faginea* Lam.

Subalpine and Alpine Zones : Characterised by the retreat of the treeline, where *Pinus uncinata* Ramond ex DC.forests transitioning into *Juniperus communis* L. scrublands and hardy alpine grasslands.

The BSM record spans approximately 9,8 ka BP, encompassing nearly the entire Holocene, with 140 pollen and 140 charcoal samples providing decadal to centennial resolution[38]. The complete list of taxa grouping into communities is available in Sec. 2 of the Supplementary Material.

*Garba Guracha (*GGU*)*

Garba Guracha is a cirque lake located at 3950 m a.s.l. on the Sanetti Plateau of the Bale Mountains National Park, Ethiopia. The site is located at the transition between the Ericaceous and afroalpine vegetation belts[39].

Afroalpine and Ericaceous Belts: Local communities are dominated by *Alchemilla haumannii* Rothm. and *Helichrysum shrublands*, transitioning into *Erica trimera* (Engl.) and *E. arborea* L. thickets.

Afromontane Forest Limit: The lower slopes feature dry afromontane forests dominated by *Juniperus procera*, *Hagenia abyssinica* (bruce), and *Podocarpus falcatus* (Thunb.) R.Br. ex Mirb.

This 15.5-metre sedimentary sequence provides a 14 ka BP record of high-altitude tropical vegetation dynamics. The GGU dataset comprises 301 pollen samples and 1301 charcoal samples, allowing for a detailed examination of fire-vegetation feedbacks. See Sec. 2 of the Supplementary Materials for the full map of taxa classified into communities.

Data metrics and processing

Palynological research frequently relies on percentages (relative abundance) estimated as the fraction of a particular taxon over the total counts of pollen grains on microscope slide. This metric is fundamentally unsuitable for causal inference due to the mathematical closure effect (*i.e.*, the sum of the percentages is always equal to 100%). In the context of Granger Causality (GC), which identifies directional predictability by testing if the history of Taxon X improves the forecast of Taxon Y, using percentages introduces severe representational biases. Under these conditions, a negative causal link may represent a mere mathematical artifact of the closure effect rather than a genuine ecological interaction, such as competition or niche partitioning.

A more accurate proxy for absolute plant biomass, is the Pollen Accumulation Rate (PAR), as it estimates the absolute rate at which pollen is deposited (also known as *influx*) per unit area per year (grains $\cdot$ cm^{-2} $\cdot$ yr^{-1}), calculated as follows:

$$\mathrm{PAR}(i) = \text{grain count} \cdot \underbrace{\frac{\text{added lycopodium spores}}{\text{counted lycopodium spores}} \cdot \frac{\text{sedimentation rate } (cm/yr)}{\text{sample volume } (cm^3)}}_{multiplier} \equiv PC(i)\ \theta(i)\ . \tag{1}$$

Lycopodium spores are an exotic marker enabling the quantitative estimation of pollen in a fossil sample as they are added to a sediment sample in a known quantity before laboratory processing. As the number of added spores is precisely controlled, they act as a reference against which the number of fossil pollen grains recovered from the sample can be compared[42]. As PAR reflects the absolute influx of pollen, it captures variations in overall vegetation productivity, sedimentation dynamics, and regional pollen rain; all of which may simultaneously affect multiple taxa. Thus, PAR serves as a reliable proxy for plant biomass[43], allowing each taxon to be tracked aside from relative fluctuations.

The use of PAR inherently assumes that all associated variables, besides pollen counts, – namely *Lycopodium* concentration, sedimentation rate, and sample volume – are known and have been accurately quantified. In practice, however, this condition is not consistently met across palaeoecological records. A central aim of this study is therefore to outline a reproducible approach applicable across diverse pollen sequences, including those where such parameters are uncertain or unavailable.

We therefore rely on pollen counts for each terrestrial taxon to infer causal relationships among taxa, as these represent the only variable that is consistently and systematically generated across palaeoecological sequences. This choice ensures comparability and broad applicability, particularly in contexts where PAR cannot be reliably estimated. Our focus on terrestrial taxa reflects the aim of reconstructing causal interactions within plant communities, where pollen counts provide a direct and internally consistent proxy for relative taxon representation through time.

To explore these causal relationships under different past scenarios of disturbance, we split the pollen counts time series of BSM and GGU into several adjacent, non-overlapping time periods, corresponding to different fire activity phases (see Fig. S2 of the Supplementary Materials). These phases correspond to internally coherent fire anomaly periods, computed as z-scores[26]. Such a procedure leads to considering different periods with distinct fire activity regimes. For BSM, we have: **period 1)** from 9.8 to 6.2 ka BP (high fire activity), **period 2)** from 6.2 to 3.8 ka BP (low fire activity), and **period 3)** from 3.8 ka BP to present time (intermediate fire activity). For GGU we have, instead: **period 1)** from 13.6 to 11.1 ka BP (low fire activity), **period 2)** from 11.1 to 6.8 ka BP (high fire activity), **period 3)** from 6.8 to 2.2 ka BP (low fire activity), and **period 4)** from 2.2 ka BP to the present (high fire activity).

The sedimentary samples are analysed homogeneously in depth, translating into a non-uniform sampling over time (*i.e.*, depth does not translate directly into time as sedimentation is not uniform). Thus, our original time series need to be interpolated to convert them into uniformly sampled temporal series. The latter step is required to use the machinery of time series analysis, which assumes that time series are evenly sampled. We used a Generalized Additive Model (GAM)[44,45] to interpolate and resample our original time series. GAM uses splines to fit the pollen abundance, and adds a penalty for smoothness ensuring the outcome is not a jagged line. It is implemented using the `GAM` function from the Python library `pyGAM`[45], leaving to the user the choice of the type of function associated with the data (note: we choose a *spline* term). GAM allows us to tune its parameters to avoid underfitting, effectively capturing our data's short-term fluctuations. The number of splines was set to the number of samples minus one, and the smoothing parameter, λ, was set to 0.01, ensuring the preservation of the perturbations which are essential to carry out statistical inference. To ensure statistical robustness, we excluded from the analysis taxa with extremely low pollen counts (*i.e.*, removing, in every time period, those time series with less than three values higher than 0.5); as their GAM interpolations correspond to close-to-zero curves, which can be assimilated to noise.

Environmental variables

Even though we are taking fire activity into account as a partitioning variable, potential relationships found in our fire-derived periods may not account for other, confounding, environmental factors. Omitting these factors may lead to artificial relationships, where multiple taxa appear to influence one another simply because they are simultaneously responding to the same external environmental factor. We have thus incorporated specific external proxies as conditional variables to –at least partially– account for some of the shared environmental drivers. This methodological approach allows us to distillate the causal relationships between taxa from the effects of external drivers acting as confounding factors, preventing false relationships from arising across the system. The integration of environmental variables differs between the two sites based on data availability. Concretely:

BSM: We used $\delta 13C$ isotope composites from Mendukillo Cave, in the Cantabrian range (Spain)[46], as a high-resolution independent reconstruction of temperature variability. By including this quantity as a conditional variable, we can distinguish genuine inter-taxa dependencies from synchronised shifts driven primarily by regional temperature changes.

GGU: Lacking an equivalent independent climate time series, with equivalent time resolution for the Ethiopian highlands, we employed PAR –*i.e.*, the multipliers, $\{\theta\}$, introduced in Eq. (1)– as primary conditional variable. By using PAR as a confounding factor, we explicitly account for the shared variance of several factors, thereby reducing spurious associations arising from compositional constraints, taphonomic biases, and common environmental drivers.

A sensitivity analysis on the effects of the *multipliers* as on the time series and variable can be found in Sec. 3 of the Supplementary Material.

Inferring causality

Granger causality

Spatial or temporal co-occurrence or co-abundance[47] does not always imply the existence of an interaction between species[48]. Causal inference is a branch of statistics aiming at determining the cause-and-effect relationship between variables, going beyond simple correlation. The standard test used to infer causality (*e.g.*, in medical trials) is the Randomized Controlled Trials (RCTs), in which we are able to manipulate the environment to find a result[49]. However, in our case, we cannot use such a method as we are compelled to use observational data in the form of time series. Therefore, we resort to observational causal discovery, which is widely used in areas such as economics and neuroscience[50,51]. This framework does not prove causal relationships in the strict philosophical sense but, rather, tests for its *predictability*. In this sense, variable X is said to mathematically *cause* variable Y if knowing the past values of X improves the prediction of Y's future values better than knowing Y's past values alone.

In observational ecology, several inference methods exist to serve this purpose, like: Structural Equation Modelling (SEM), Empirical Dynamic Modeling (EDM), Bayesian networks, Transfer Entropy (TE), and Granger Causality (GC)[52–54]. We choose the latter to test for causal relationships between pairs of taxa. The GC compares two Vector Autoregressive Models (VARs): the unrestricted (in which both the *caused* and *causing* taxon's past values are taken into account) and and restricted (in which

only the *caused* taxon's past values taken into account). Additionally, these VAR models allow to introduce external (*i.e.*, *conditional*) variables to account for confounding factors that could explain some of the observed causal links. Given two time series $X \equiv \{X_1, \ldots, X_T\}$ and $Y \equiv \{Y_1, \ldots, Y_T\}$, and indicating their values at time t as X_t and Y_t, the unrestricted Granger Causality model is written as:

$$Y_t = c_0 + \sum_{i=1}^{h} \alpha_i X_{t-i} + \sum_{j=1}^{h} \beta_j Y_{t-j} + \sum_{p} \sum_{k=1}^{h} \gamma_k^p C_{t-k}^p + u_t \ , \tag{2}$$

where c_0 is the intercept, β_i are the variable Y (*i.e.*, *caused*) own-lagged coefficients, α_i are the (*causing*) variable X cross-lagged coefficients, and γ_k^p are the cross-lagged coefficients of the *conditional* variables C^p[52]. Additionally, u_t are the residuals, which are assumed to have a normal distribution (*i.e.*, a white noise). Lastly, h is the maximum time lag, which we set to one to avoid overfitting, given the limited number of data points. Under the assumption that $h = 1$, β_1 represents the autocorrelation component of the time series Y, whereas α_1 is the cross-lagged coefficient and accounts for the effect that X has on Y. This value has no bounds, as it depends on the relative scale of both series and we are required to test its significance through an F-Statistic or against a null model.

Bootstrapping

In principle, the residuals u_t can be used to compute the F-Statistic of the GC's values to estimate theoretically the p-value to determine whether a causal relationship between two variables exists (*i.e.*, it is statistically significant) or not. However, the necessary mathematical assumptions behind such an approach rarely hold true when dealing with empiric data. The use of *bootstrapping* is a valid alternative to verify the causality test's null hypothesis, and estimate then the p-values for all pairs of variables[55]. In particular, bootstrapping addresses several issues: i) small sample sizes (as the F-Statistic relies on asymptotic theory and assumes infinite data points), ii) the assumption of normally distributed residuals, iii) the data's autocorrelation, and iv) the evolution over time in the variance of non-stationary series. Overall, the p-values estimated via bootstrapping are less skewed towards lower (*i.e.*, more statistically significant) values than the theoretical ones. Among the several methods available, we chose the so-called *stationary bootstrap*[55,56].

Stationary bootstrap resamples contiguous blocks of data from the original series of length, T, to generate a new series by pasting blocks of random lengths $t_i' < T$ until getting a series whose size is equal to the original (*i.e.*, $\sum_i t_i' = T' = T$). Stationary bootstrap, unlike the so-called independent and identically distributed (IDD) bootstrapping, has the advantage of preserving the data's autocorrelation[51,56].

For every pair of taxa in our datasets, we resampled the time series 1,000 times and obtained their respective causality coefficient α_1. Then, for each pair of taxa (i, j) the p-value associated with $\mathrm{GC}(i, j)$ indicates the proportion of bootstrapped tests for which the condition $\left|\mathrm{GC}'(i, j)\right| > \left|\mathrm{GC}(i, j)\right|$ holds (*i.e.*, the GC in the bootstrapped pair has a higher absolute value than the empirical one).

Causality networks

The versatility of network science allows its application to many disciplines, from social sciences[57] to physical systems[58], from neuroscience[59] to biology and ecology[60]. We represent the causal relationships between taxa as a *causal network* (or graph), $G(\mathscr{N}, \mathscr{E})$[61,62]. In such a network, nodes are the taxa, and a link between taxa i and j, $(i, j) \in \mathscr{E}$ denotes a statistically significant causal relationship between them (*i.e.*, the p-value of $\mathrm{GC}(i, j)$ is less or equal to 0.05, see Eq. (2)). Given the intrinsic nature of the GC, the links of G are directed, signed, and weighted; with the second corresponding to the sign of the GC (*i.e.*, $s(i, j) = \frac{\mathrm{GC}(i,j)}{|\mathrm{GC}(i,j)|}$), and the latter denoting its value (*i.e.*, $w(i, j) = |\mathrm{GC}(i, j)|$).

We built a causality network for each time period in our datasets (*i.e.*, three for BSM and four for GGU). In the following, we describe several fundamental macroscopic measures of our networks. For instance, the *degree* of a node is equal to the number of links incident with it. As links have a direction, the degree splits into its *in-ward* and *out-ward* components. A connected component is a set of nodes which can be reached from each other via a sequence of links (*i.e.*, a path)[61]. The size of the *Giant Connected Component* (GCC) of the network is defined as the number of nodes belonging to the biggest connected component, N_{GCC}, divided by the total number of nodes in the network, N.

Beside the network of causal relationships between taxa, one can study also its *coarse-grained* counterpart, *i.e.*, a new network mapping the original one, $G(\mathscr{N}, \mathscr{E})$, (with N nodes and E links) into a smaller one, $G'(\mathscr{N}', \mathscr{E}')$, (such that $N' < N$ and $E' < E$). Several coarse-graining methods exist (see, for instance Gfeller *et al.*[63] and references therein) but, we decided to use a custom one. Specifically, to give more sense to the web of interactions, and map them onto known ecological communities, we grouped the taxa into *communities* (*e.g.*, pastureland) designated by an expert (see Sec. 2 of the Supplementary Materials for the details). In our coarse network a link between two communities, a and b, $(a, b) \in \mathscr{E}'$ denotes the existence of links between taxa belonging to these communities. In agreement with the original network, G, the links of G' are also directed, signed, and

weighted. Although the first two properties map directly between graphs, the weight of a link in G', w', does not indicate the value of the GC but, instead, the number of statistically significant links existing between taxa belonging to two communities. Moreover, the network G' possesses links beginning/ending in the same community (*i.e.*, self-loops, E_0), encoding the existence of relationships between taxa belonging to the same community.

Network temporality

The temporality of a network represents the volatility of its connections, giving us a sense of the persistence of the relationships between causal relationships over time. Given a pair of networks G_i and G_{i+1}, we define the network temporality between them, $\mathscr{T}_{G_i,G_{i+1}}$ as the Jaccard distance between their links' sets[64], yielding:

$$\mathscr{T}_{G_i,G_{i+1}} = 1 - \frac{\text{Common links of } G_i \text{ and } G_{i+1}}{\text{All links of } G_i \text{ and } G_{i+1}},$$

where the numerator denotes the number of links existing in both Period i and Period $i+1$, whereas the denominator is the number of links that exist in either one or the other (or both). A value of $\mathscr{T}_{G_i,G_{i+1}} = 1$ indicates that networks G_i and G_{i+1} have no links in common, whereas a value of $\mathscr{T}_{G_i,G_{i+1}} = 0$ indicates that the two networks have exactly the same links.

Additional methodological remarks in connection with the causal inference method selection, read the methodological remarks in the Supplementary Material.

Acknowledgments

AC, PV, CRC, PGS, and GGR acknowledge financial support from the Spanish Agency for Research (AEI) and the Ministerio de Ciencia e Innovación, through project CORREDORAS No. PID2022-141558NB-I00. AC acknowledges financial support from the Spanish Ministerio de Ciencia e Innovación, through project PID2024-158120NB-C22, and from the Ramón y Cajal program (Agencia Estatal de Investicación) through the grant no. RYC2023-044587-I.

The authors thank also M. Chavez, V. Calleja-Solanas, and O. Godoy for helpful discussions and M. Sevilla-Callejo for providing Fig. 1.

Author contributions statement

GGR, PGS, and HS conceptualized the study. GGR, PGS, and CRC curated the data. AC, PV, ATC, DCG, HS, and GGR discussed the methodology. PV and AC performed the simulations, curated the code, and visualizations. GGR, PV, and AC analysed the results. GGR, PV, and AC wrote the first draft. All authors contributed to the results discussion, read, reviewed, and approved the final manuscript.

Additional information

Competing interests The authors declare no competing interests.

Availability of data and materials @@@@@ DATA AVAILABILITY @@@@@

Ethical approval This article does not contain any studies with human participants performed by any of the authors.

Informed consent This article does not contain any studies with human participants performed by any of the authors.

References

1. Chesson, P. Updates on mechanisms of maintenance of species diversity. *J. Ecol.* **106**, 1773–1794, DOI: 10.1111/1365-2745.13035 (2018).
2. Rockström, J. *et al.* A safe operating space for humanity. *Nature* **461**, 472–475, DOI: 10.1038/461472a (2009).
3. Duane, A., Castellnou, M. & Brotons, L. Towards a comprehensive look at global drivers of novel extreme wildfire events. *Clim. Chang.* **165**, 43, DOI: 10.1007/s10584-021-03066-4 (2021).
4. He, T., Lamont, B. B. & Pausas, J. G. Fire as a key driver of Earth's biodiversity. *Biol. Rev.* **94**, 1983–2010, DOI: 10.1111/brv.12544 (2019).
5. Keeley, J. E., Pausas, J. G., Rundel, P. W., Bond, W. J. & Bradstock, R. A. Fire as an evolutionary pressure shaping plant traits. *Trends Plant Sci.* **16**, 406–411, DOI: 10.1016/j.tplants.2011.04.002 (2011).

6. Valiente-Banuet, A. & Verdú, M. Temporal shifts from facilitation to competition occur between closely related taxa. *J. Ecol.* **96**, 489–494, DOI: 10.1111/j.1365-2745.2008.01357.x (2008).

7. Chozas, S. *et al.* Dynamics of post fire plant community assembly in Doñana coastal dunes. *Sci. Reports* **15**, DOI: 10.1038/s41598-025-04400-x (2025).

8. Hollingsworth, T. N., Johnstone, J. F., Bernhardt, E. L. & Chapin, F. S., III. Fire Severity Filters Regeneration Traits to Shape Community Assembly in Alaska's Boreal Forest. *PLOS ONE* **8**, 1–11, DOI: 10.1371/journal.pone.0056033 (2013).

9. Weiher, E. & Keddy, P. (eds.) *Ecological Assembly Rules: Perspectives, Advances, Retreats* (Cambridge University Press, 1999).

10. Fraterrigo, J. M., Langille, A. B. & Rusak, J. A. Stochastic disturbance regimes alter patterns of ecosystem variability and recovery. *PLOS ONE* **15**, 1–20, DOI: 10.1371/journal.pone.0229927 (2020).

11. Romme, W. H., Whitby, T. G., Tinker, D. B. & Turner, M. G. Deterministic and stochastic processes lead to divergence in plant communities 25 years after the 1988 Yellowstone fires. *Ecol. Monogr.* **86**, 327–351, DOI: 10.1002/ecm.1220 (2016).

12. Woodhouse, A. *et al.* The Micropaleoecology Framework: Evaluating Biotic Responses to Global Change Through Paleoproxy, Microfossil, and Ecological Data Integration. *Ecol. Evol.* **14**, e70470, DOI: 10.1002/ece3.70470 (2024).

13. Manzano, S. *et al.* Using the past to manage the future: The role of palaeoecological and long-term data in ecological restoration. *Restor. Ecol.* **28**, DOI: 10.1111/rec.13285 (2020).

14. Moreno-Mateos, D. *et al.* The long-term restoration of ecosystem complexity. *Nat. Ecol. & Evol.* **4**, 676–685, DOI: 10.1038/s41559-020-1154-1 (2020).

15. Carpenter, S., Walker, B., Anderies, J. M. & Abel, N. From Metaphor to Measurement: Resilience of What to What? *Ecosystems* **4**, 765–781, DOI: 10.1007/s10021-001-0045-9 (2001).

16. Chesson, P. Mechanisms of Maintenance of Species Diversity. *Annu. Rev. Ecol. Evol. Syst.* **31**, 343–366, DOI: 10.1146/annurev.ecolsys.31.1.343 (2000).

17. Holdridge, E. M. & Vasseur, D. A. Intraspecific Variation Promotes Coexistence under Competition for Essential Resources. *Theor. Ecol.* **15**, 225–244, DOI: 10.1007/s12080-022-00539-9 (2022).

18. Kunze, C. *et al.* Partitioning species contributions to ecological stability in disturbed communities. *Ecol. Monogr.* **95**, e1636, DOI: 10.1002/ecm.1636 (2025).

19. Zhang, H. *et al.* Multiple stressors drive multitrophic biodiversity and ecological network dynamics in a shrinking sandy lake. *Commun. Earth & Environ.* **5**, 527, DOI: 10.1038/s43247-024-01704-0 (2024).

20. Sutton, L., Mueter, F. J., Bluhm, B. A. & Iken, K. Environmental Filtering Influences Functional Community Assembly of Epibenthic Communities. *Front. Mar. Sci.* **8**, DOI: 10.3389/fmars.2021.736917 (2021).

21. Furniss, T. J., Larson, A. J. & Lutz, J. A. Reconciling niches and neutrality in a subalpine temperate forest. *Ecosphere* **8**, e01847, DOI: 10.1002/ecs2.1847 (2017).

22. Kaiser-Bunbury, C. N. *et al.* Ecosystem restoration strengthens pollination network resilience and function. *Nature* **542**, 223–227, DOI: 10.1038/nature21071 (2017).

23. Barraquand, F., Picoche, C., Detto, M. & Hartig, F. Inferring species interactions using Granger causality and convergent cross mapping. *Theor. Ecol.* **14**, 87–105, DOI: 10.1007/s12080-020-00482-7 (2021).

24. García, M. B. *et al.* Habitats hold an evolutionary signal of past climatic refugia. *Biodivers. Conserv.* **31**, 1665–1688, DOI: 10.1007/s10531-022-02419-4 (2022).

25. Freeman, B. G., Flantua, S. G. A., Feeley, K. J., McCain, C. M. & McGuire, J. L. The fate of mountain biodiversity in a warming world. *Nat. Rev. Biodivers.* 1–16, DOI: 10.1038/s44358-026-00167-9 (2026).

26. Leunda, M., Gil-Romera, G., Daniau, A.-L., Benito, B. M. & González-Sampériz, P. Holocene fire and vegetation dynamics in the Central Pyrenees (Spain). *CATENA* **188**, 104411, DOI: https://doi.org/10.1016/j.catena.2019.104411 (2020).

27. Gil-Romera, G. *et al.* Long-term fire resilience of the Ericaceous Belt, Bale Mountains, Ethiopia. *Biol. Lett.* **15**, 20190357, DOI: 10.1098/rsbl.2019.0357 (2019).

28. Villar Pérez, L., Sesé Franco, J. A. & Ferrández Palacio, J. V. *Atlas de la flora del Pirineo aragonés*, vol. 1 (Consejo de Protección de la Naturaleza de Aragón, 1997).

29. Hedberg, O. Altitudinal zonation of the vegetation on the East African mountains. *Proc. Linnean Soc. Lond.* **165**, 134–136, DOI: 10.1111/j.1095-8312.1955.tb00730.x (1955).

30. Bittner, L. *et al.* The Holocene lake-evaporation history of the afro-alpine Lake Garba Guracha in the Bale Mountains, Ethiopia, based on d18O records of sugar biomarker and diatoms. *Quat. Res.* 1–14, DOI: 10.1017/qua.2021.26 (2021).

31. Bittner, L. *et al.* A Holocene temperature (brGDGT) record from Garba Guracha, a high-altitude lake in Ethiopia. *Biogeosciences* **19**, 5357–5374, DOI: 10.5194/bg-19-5357-2022 (2022).

32. Barabás, G., D'Andrea, R. & Stump, S. M. Chesson's coexistence theory. *Ecol. Monogr.* **88**, 277–303, DOI: 10.1002/ecm.1302 (2018).

33. HilleRisLambers, J., Adler, P., Harpole, W., Levine, J. & Mayfield, M. Rethinking Community Assembly through the Lens of Coexistence Theory. *Annu. Rev. Ecol. Evol. Syst.* **43**, 227–248, DOI: 10.1146/annurev-ecolsys-110411-160411 (2012).

34. Gil-Romera, G. *et al.* Biomass-modulated fire dynamics during the Last Glacial–Interglacial Transition at the Central Pyrenees (Spain). *Palaeogeogr. Palaeoclimatol. Palaeoecol.* **402**, 113–124, DOI: 10.1016/j.palaeo.2014.03.015 (2014).

35. HilleRisLambers, J., Adler, P. B., Harpole, W. S., Levine, J. M. & Mayfield, M. M. Rethinking Community Assembly through the Lens of Coexistence Theory. *Annu. Rev. Ecol. Evol. Syst.* **43**, 227–248, DOI: 10.1146/annurev-ecolsys-110411-160411 (2012).

36. Godoy, O. Coexistence theory as a tool to understand biological invasions in species interaction networks: Implications for the study of novel ecosystems. *Funct. Ecol.* **33**, 1190–1201, DOI: 10.1111/1365-2435.13343 (2019).

37. Calleja-Solanas, V., Bartomeus, I. & Godoy, O. Time-varying interactions drive species coexistence via rainfall variation. *bioRxiv* DOI: 10.1101/2025.11.28.690940 (2025). https://www.biorxiv.org/content/early/2025/12/01/2025.11.28.690940.full.pdf.

38. Pérez-Sanz, A. *et al.* Holocene Climate Variability, Vegetation Dynamics and Fire Regime in the Central Pyrenees: The Basa de La Mora Sequence (NE Spain). *Quat. Sci. Rev.* **73**, 149–169, DOI: 10.1016/j.quascirev.2013.05.010 (2013).

39. Gil-Romera, G. *et al.* The new Garba Guracha palynological sequence: Revision and data expansion. In *Quaternary Vegetation Dynamics*, 127–134, DOI: 10.1201/9781003162766 (CRC Press, 2021).

40. Villar Pérez, L., Sesé Franco, J. A. & Ferrández Palacio, J. V. *Atlas de la flora del Pirineo aragonés*, vol. 2 (Consejo de Protección de la Naturaleza de Aragón, 2001).

41. Miehe, S. & Miehe, G. *Ericaceous Forests and Heathlands in the Bale Mountains of South Ethiopia: Ecology and Man's Impact* (Warnke, 1994).

42. Stockmarr, J. Determination of spore concentration with an electronic particle counter. In *DGU Årbog 1972*, vol. 1972, 87–89, DOI: 10.22008/gpub/38152 (DGU, 1973).

43. Seppä, H. *et al.* Calibrated pollen accumulation rates as a basis for quantitative tree biomass reconstructions. *The Holocene* **19**, 209–220, DOI: 10.1177/0959683608100565 (2009).

44. Hastie, T. & Tibshirani, R. Generalized Additive Models. *Stat. Sci.* **1**, 297–318 (1986).

45. Servén, D. *et al.* pyGAM: v0.10.1. Zenodo, DOI: 10.5281/zenodo.16453423 (2025).

46. Bernal-Wormull, J. L. *et al.* New insights into the climate of northern Iberia during the Younger Dryas and Holocene: The Mendukilo multi-speleothem record. *Quat. Sci. Rev.* **305**, 108006, DOI: 10.1016/j.quascirev.2023.108006 (2023).

47. Cazelles, K., Araújo, M. B., Mouquet, N. & Gravel, D. A theory for species co-occurrence in interaction networks. *Theor. Ecol.* **9**, 39–48, DOI: 10.1007/s12080-015-0281-9 (2016).

48. Coenen, A. R. & Weitz, J. S. Limitations of Correlation-Based Inference in Complex Virus-Microbe Communities. *mSystems* **3**, 10.1128/msystems.00084–18, DOI: 10.1128/msystems.00084-18 (2018).

49. Rubin, D. Estimating causal effects of treatments in experimental and observational studies. *ETS Res. Bull. Ser.* **1972**, i–31, DOI: https://doi.org/10.1002/j.2333-8504.1972.tb00631.x (1972).

50. Kumar, S., Vivek, Y., Ravi, V. & Bose, I. A Comprehensive Review of Causal Inference in Banking, Finance, and Insurance. *ACM Comput. Surv.* **57**, DOI: 10.1145/3736752 (2025).

51. Chávez, M., Martinerie, J. & Le Van Quyen, M. Statistical assessment of nonlinear causality: application to epileptic EEG signals. *J. Neurosci. Methods* **124**, 113–128, DOI: 10.1016/S0165-0270(02)00367-9 (2003).

52. Granger, C. W. J. Investigating Causal Relations by Econometric Models and Cross-spectral Methods. *Econometrica* **37**, 424–438, DOI: 10.2307/1912791 (1969).

53. Correia, H. E. *et al.* Best practices for moving from correlation to causation in ecological research. *Nat. Commun.* **17**, 1981, DOI: 10.1038/s41467-026-69878-z (2026).

54. Krakovská, A. *et al.* Comparison of six methods for the detection of causality in a bivariate time series. *Phys. Rev. E* **97**, 042207, DOI: 10.1103/PhysRevE.97.042207 (2018).

55. Lahiri, S. N. *Resampling Methods for Dependent Data*. Springer Series in Statistics (Springer New York, New York, NY, 2003).

56. Politis, D. N. & Romano, J. P. The Stationary Bootstrap. *J. Am. Stat. Assoc.* **89**, 1303–1313, DOI: 10.1080/01621459.1994.10476870 (1994).

57. Wasserman, S. & Faust, K. *Social Network Analysis: Methods and Applications*. Structural Analysis in the Social Sciences (Cambridge University Press, Cambridge, 1994).

58. Barabási, A.-L. The network takeover. *Nat. Phys.* **8**, 14–16, DOI: 10.1038/nphys2188 (2012).

59. Sporns, O. *Networks of the Brain* (MIT Press, Cambridge, MA, USA, 2016).

60. Pilosof, S., Porter, M. A., Pascual, M. & Kéfi, S. The multilayer nature of ecological networks. *Nat. Ecol. & Evol.* **1**, DOI: 10.1038/s41559-017-0101 (2017).

61. Latora, V., Nicosia, V. & Russo, G. *Complex Networks: Principles, Methods and Applications* (Cambridge University Press, Cambridge, 2017).

62. Runge, J. Causal network reconstruction from time series: From theoretical assumptions to practical estimation. *Chaos: An Interdiscip. J. Nonlinear Sci.* **28**, 075310, DOI: 10.1063/1.5025050 (2018).

63. Gfeller, D. & De Los Rios, P. Spectral Coarse Graining of Complex Networks. *Phys. Rev. Lett.* **99**, 038701, DOI: 10.1103/PhysRevLett.99.038701 (2007).

64. Bauzá Mingueza, F., Floría, M., Gómez-Gardeñes, J., Arenas, A. & Cardillo, A. Characterization of interactions' persistence in time-varying networks. *Sci. Reports* **13**, 765, DOI: 10.1038/s41598-022-25907-7 (2023).